**DTU Library**

# Resonant inerter based vibration absorbers on flexible structures

**Krenk, Steen**

Link back to DTU Orbit

# Resonant inerter based vibration absorbers on flexible structures

Steen Krenk

*Department of Mechanical Engineering,*
*Technical University of Denmark, DK-2800 Lyngby, Denmark*

**Abstract**

The paper presents an explicit two-step calibration procedure for tuned inerter based vibration absorbers on flexible structures. It makes use of a local approximate representation of the structural response to the device force, in which the contribution of the non-resonant modes is represented approximately around the resonance frequency by a background flexibility and a background inertia term. The calibration procedure then consists of two steps. The first step calibrates an equivalent vibration absorber including the background terms, and the second step subsequently evaluates the parameters of the actual device by extracting the background flexibility and inertia parameters. The first step represents the classic idealized single degree of freedom representation of the structure, whereas the second step leads to an increase of stiffness, inertia and damping parameters of the actual device due to background flexibility of the structure. The procedure is illustrated in detail for three inerter based vibration absorbers: parallel coupling of damper and stiffness, parallel coupling of damper and inerter, and finally a device with two dampers in parallel with stiffness and inerter elements, respectively. Explicit expressions for the calibration are obtained for each device, and it is demonstrated that the procedure leads to a balanced plateau of amplification around the resonance frequency of the magnitude assumed as the basis for the device parameter calibration.

*Keywords:* Vibration damping, Inerter absorber, Absorber calibration, Non-resonant modes, Structural dynamics.

## 1. Introduction

The basic mechanism of vibration damping is extraction of energy, and if the desired damping is associated with a particular mode a device in resonance with this mode enables higher efficiency. The classic example is the tuned mass absorber in which a vibrating mass is supplemented by an additional device mass that is attached through a spring and a damper as described e.g. by Den Hartog [1]. The design problem of this idealized structure consists in selecting a suitable tuning frequency and a suitable damper in the device. The classic design procedure is based on a frequency plot the dynamic amplification factor, and typically involves frequency tuning to place two characteristic fixed points at the same level of amplification, and then selecting a suitable level of

damping to attain a fairly level plateau between the two fixed points, typically by the procedure proposed by Brock [2]. The tuned mass absorber operates with the absolute motion of the device mass. Much more recently an alternative form of a mechanical vibration absorber was proposed by Smith [3] in which the inertial term is generated from the relative motion of two points through a so-called inerter. The principle as well as various device configurations have been discussed by Chen et al. [4]. Theoretically inerter based vibration absorbers have extensive similarities with electromechanical devices, and these can in fact be explored via the classic analogies between the mechanics of spring, inerter and damping elements, and the electronic properties of inductor, capacitor and resistor components, as discussed in [4], and by Alessandroni et al. [5] and Zhu et al. [6]. In the present paper all derivations will be presented directly for mechanical inerter based devices.

The classic design procedure in terms of properties of the dynamic amplification curve was replaced by a root locus based procedure by Krenk [7], where it was demonstrated that the classic equal amplification of two fixed points is equivalent to two roots with equal damping, and the damping ratio was determined by a direct condition of maximum flatness of the dynamic amplification curve. The 'equal damping' calibration procedure contains the classic three-component mass or inerter based devices as a special case but also applies to other device configurations as demonstrated e.g. in the present paper. The key point is the property of equal modal damping – obtained by suitable frequency tuning – leading to a form of the quartic characteristic equation that can be reformulated to quadratic form, thereby permitting a fairly simple solution with a direct connection between the device parameters and the response properties. Further root locus analyses were presented by Bisegna and Caruso [8].

The classic formulations of the theory for tuned mass or inerter based absorbers typically assume the main structure is undamped, because including damping in the structure complicates the harmonic dynamic equations and seems to prevent simple analytical results for calibration of the device. In the case of random loading the situation is reversed. Now, it is convenient to include damping of the primary structure, because the spectral moments of the response in the absence of the device would otherwise not be available. The basic problem of a single-mass damped structure equipped with a tuned mass device was treated by Bakre and Jagid [9], Krenk and Høgsberg [10] and Tigli [11] for white noise base or force excitation of the main system, equivalent to use of the $H_2$-norm for the response variances. The results for response variances are quite complicated and the resulting optimal frequency tuning and device damping parameters similarly involved and quite difficult to obtain. Part of the complication is due to the fact that the optimal values of the frequency ratio now depends on both structure and device damping ratios. Additionally, the white noise excitation changes the optimal frequency ratio, even in the absence of structural damping. This shift of optimal frequency is due to the effect of the high-frequency spectral components implied by the white-noise assumption. As demonstrated in [10] the results simplify considerably if neglecting this frequency shift and tuning the system to the classic harmonic excitation frequency. Furthermore, the resulting explicit damping approximation fits the numerically computed values quite well. A similar analysis of an inerter based single-degree-of-freedom system was recently presented in Pan and Zhang [12]. Hu and Chen [13] extended the basic device format to four inerter based resonant device configurations and presented results from $H_2$-norm

2

optimization. A different angle on the random excitation problem was given by Zilletti et al. [14], who considered the power input and demonstrated that maximizing the dissipation rate of the absorber corresponds to minimizing the kinetic energy of the structure. Finally, the extension to a device with non-linear damping by Shum [15] should be mentioned.

The potential of the inerter as a replacement of the mass element in a similar tuned mass configuration has been demonstrated for base excitation of buildings by Lazar et al. [16] and the extended problem of simultaneous use of multiple inerter based damping devices on a building by Wen et al. [17]. The damping of a cable by a similar discrete model with an inerter based damping device was investigated by Lazar et al. [18]. An alternative formulation of the inerter based damper on a cable was used by Sun et al. [19] and Shi and Zhu [20], who extended the analytical solution for a viscous damper [21] to a resonant inerter based device and obtained detailed root locus information of several modes.

Tuned inerter based devices permit more combinations of the components than the classic tuned mass absorber. One of these combinations, proposed by Marian and Giaralis [22], consists of a classic three-component tuned mass device coupled in series with an inerter. The combined four-component TMDI device connects two points on the structure and thereby has the form of a generalized inerter based vibration absorber. Its efficiency and use have also been investigated by Giaralis and Petrini [23] and De Domenico and Ricciardi [24]. The series coupling is theoretically closely related to the background inertia term as discussed in the present paper. More general network variations of inerter based devices have been proposed by Zhang et al. [25] including the coupling of two full three-component inerter based devices of which one is parallel with an inerter. The demonstration example includes a flexible supporting brace – an effect that can be accounted for by a series coupled flexibility in the procedure discussed here.

The papers mentioned above deal with individual devices or devices interacting with an idealized structure, represented by a selected resonant mode. In reality the device represents a local set of forces on the structure and therefore in principle interacts with all the vibration modes. However, in practice for calibration purposes the deformation of the structure, corresponding to the relative displacement of the two terminals of the device, can often be approximated to a fairly high degree of accuracy by a contribution from the resonant mode plus a contribution from local deformation. The situation to some degree resembles the classic approximation in which a modal analysis of a structure is limited to a set of the lower modes, while the higher modes are represented by their quasi-static contributions, see e.g. Maddox [26] and Hansteen and Bell [27]. This formulation was recast into the representation of the local deformation at the terminal of a tuned mass absorber as the sum of a modal and a local quasi-static contribution, Krenk and Høgsberg [28]. The quasi-static representation of the deformation from non-resonant modes limits this formulation to cases where the resonant mode is the lowest, or with only lower modes orthogonal to the device forces. A more general quasi-dynamic representation was developed in Krenk and Høgsberg [29] and presented for tuned mass and inerter absorbers. This procedure was developed for passive shunt damping in Høgsberg and Krenk [30].

The present paper presents a two step method for calibration of some basic resonant inerter based vibration absorbers mounted on a flexible structure. In the first step a

3

preliminary determination of the device parameters is made, based on the 'equal modal damping' procedure for the complex characteristic equation of a device interacting with a single-degree-of-freedom system. These parameters are then modified to account for additional deformation at the location of the device due to the effect of non-resonant modes. It is demonstrated that this procedure effectively leads to equal amplification at the two peaks around resonance and a simple design procedure permitting prescribing the target amplification is described. The key steps in this procedure are presented in tabular format for three inerter based devices.

## 2. Flexible structure with vibration absorber

The structure is defined by its stiffness, mass and viscous damping matrices $\mathbf{K}$, $\mathbf{M}$ and $\mathbf{C}$, respectively. The motion of the structure is described by the displacement vector $\mathbf{u}$, satisfying the equation of motion

$$\mathbf{M\ddot{u}} + \mathbf{C\dot{u}} + \mathbf{Ku} + \mathbf{f}_d = \mathbf{f}_e, \tag{1}$$

where $\mathbf{f}_e$ is the external load, and $-\mathbf{f}_d$ is the load exerted on the structure by the local device. This corresponds to a total load $\mathbf{f} = \mathbf{f}_e - \mathbf{f}_d$ on the structure. While analysis of response of the structure and the device is conveniently based directly on the equation of motion (1) the calibration of the device depends on the frequency response around the targeted resonance frequency and is carried out via a modal analysis.

### 2.1. Modal response representation

The calibration of the device is based on a modal analysis of the undamped structure in which the response and forces are assumed implicitly to contain the time variation factor $\exp(i\omega t)$. Hereby $\mathbf{u}$ and $\mathbf{f}$ represent the corresponding amplitudes, related by the frequency equation

$$[\mathbf{K} - \omega^2\mathbf{M}]\mathbf{u} = \mathbf{f}. \tag{2}$$

The eigenfrequencies $\omega_j$ and the corresponding mode shape vectors $\mathbf{u}_j$ are determined from the corresponding homogeneous equation

$$[\mathbf{K} - \omega_j^2\mathbf{M}]\mathbf{u}_j = \mathbf{0}, \quad j = 1, \cdots, n \tag{3}$$

where $n$ is the number of degrees-of-freedom of the structural system. When introducing a representation of the response $\mathbf{u}$ in terms of the mode shape vectors $\mathbf{u}_j$ the solution to (2) is found in the form

$$\mathbf{u} = \Big[ \sum_{j=1}^{n} \frac{\omega_j^2}{\omega_j^2 - \omega^2} \frac{\mathbf{u}_j\mathbf{u}_j^T}{\mathbf{u}_j^T\mathbf{K}\mathbf{u}_j} \Big] \mathbf{f}. \tag{4}$$

This formula contains $n$ terms and a central part of the calibration procedure is to use a simplified approximate form that permits analytical solution of the corresponding characteristic equation.

The calibration procedure considers a load corresponding to the forces from the device acting on the structure. As illustrated in Fig. 1 the device connects two degrees
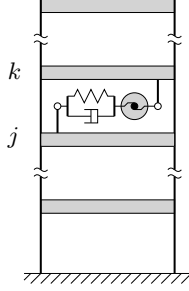
Figure 1: Structure with resonant inerter device.

of freedom of the structure and the corresponding displacement and force can therefore be expressed in terms of an integer array of the form $\mathbf{w} = [\,0, 0, -1, \cdots, 1, 0\,]$ by the relations

$$u = \mathbf{w}^T \mathbf{u}, \qquad \mathbf{f} = \mathbf{w}\, f. \tag{5}$$

When using these relations in (4), the local response relation takes the form

$$u = -\Big[\, \sum_{j=1}^{n} \frac{\omega_j^2}{\omega_j^2 - \omega^2} \frac{1}{k_j} \,\Big] f\,, \tag{6}$$

where $1/k_j$ is the modal flexibility

$$\frac{1}{k_j} = \frac{(\mathbf{w}^T \mathbf{u}_j)^2}{\mathbf{u}_j^T \mathbf{K} \mathbf{u}_j}\,, \tag{7}$$

corresponding to the mode shape vector $\mathbf{u}_j/(\mathbf{w}^T \mathbf{u}_j)$, normalized to unity at the device.

*2.2. Single resonant mode representation with stiffness and inertia terms*

In the calibration of the device for damping vibrations around a selected resonant frequency $\omega_r$ it is desirable to represent the structural response around the resonant frequency as the sum of the resonant response of mode $r$, plus a suitable simplified representation of the response from the non-resonant modes, $j \neq r$,

$$u = \Big[\, \frac{\omega_r^2}{\omega_r^2 - \omega^2} \frac{1}{k_r} + \sum_{j \neq r} \frac{\omega_j^2}{\omega_j^2 - \omega^2} \frac{1}{k_j} \,\Big] f. \tag{8}$$

The task is to find an approximate representation of sum of the non-resonant terms that permits explicit calibration of the device parameters. The simplest procedure is to neglect the non-resonant terms in the calibration. This is the classic single-mode representation. Its accuracy depends on the location of the device, and in many cases it may be difficult, or undesirable, to mount the device at points at which the response contributions from the non-resonant modes are negligible. If the resonant mode is the lowest, corresponding to $r = 1$, the non-resonant modes will have higher frequencies,

and it may be sufficient to replace the summation by a constant $1/k_r^0$, corresponding to a background stiffness, [28]. Recently, an improved representation of the effect of the non-resonant modes has been derived [29], in which sum of the non-resonant contributions is represented by a stiffness term plus an inertia term, resulting in the approximate response relation

$$u \simeq \left[ \frac{\omega_r^2}{\omega_r^2 - \omega^2} \frac{1}{k_r} + \frac{1}{k_r'} - \frac{1}{m_r'} \frac{1}{\omega^2} \right] f. \tag{9}$$

The parameters $k_r'$ and $m_r'$ are determined to give the correct full response and the correct frequency derivative at $\omega = \omega_r$. It is an important point of this representation, that it provides an accurate description of the response in a frequency range around the resonant frequency $\omega_r$, used in the device calibration procedure, and that the stiffness and inertia parameters $k_r'$ and $m_r'$ can be evaluated from the structure stiffness and mass matrices $\mathbf{K}$ and $\mathbf{M}$ without a complete eigenvalue analysis as outlined below. The coefficients $k_r'$ and $m_r'$ are properties of the structure and independent of any particular properties of the device apart from the points of attachment. It is interesting to note that the isolated effect of the flexibility of a connecting brace considered in [25] can be included directly as an additive contribution to the flexibility $1/k_r'$, and the extra series-coupled inerter element in the four-component resonant vibration absorber considered in [22, 23, 24] can be included in the present analysis as an additive contribution to $1/m_r'$.

The first step is to represent each term in the summation in (8) by an approximate expression of the form $A_j + B_j/\omega^2$, and then to determine the coefficients $A_j$ and $B_j$ from the conditions of value and slope at $\omega = \omega_r$. The result is the approximate representation

$$\frac{\omega_j^2}{\omega_j^2 - \omega^2} \simeq \frac{\omega_j^4}{(\omega_j^2 - \omega_r^2)^2} - \frac{\omega_j^2 \omega_r^2}{(\omega_j^2 - \omega_r^2)^2} \frac{\omega_r^2}{\omega^2}, \tag{10}$$

for $j \neq r$. With this expression the background stiffness and inertia parameters $k_r'$ and $m_r'$ are determined by the sums

$$\frac{1}{k_r'} = \sum_{j \neq r} \frac{\omega_j^4}{(\omega_j^2 - \omega_r^2)^2} \frac{1}{k_j}, \qquad \frac{1}{\omega_r^2 m_r'} = \sum_{j \neq r} \frac{\omega_j^2 \omega_r^2}{(\omega_j^2 - \omega_r^2)^2} \frac{1}{k_j}. \tag{11}$$

It follows from these expressions that both the background stiffness $k_r'$ and the background inertia $m_r'$ are positive. Direct relations, avoiding evaluation of modal properties, apart from the resonant frequency $\omega_r$ and mode shape $\mathbf{u}_r$, are obtained by appropriate series representation of the system matrices.

It is easily verified that the stiffness matrix $\mathbf{K}$ can be expanded in terms of the eigenvectors $\mathbf{u}_j$ as

$$\mathbf{K} = \sum_{j=1}^{n} \frac{(\mathbf{K}\mathbf{u}_j)(\mathbf{u}_j^T \mathbf{K})}{\mathbf{u}_j^T \mathbf{K}\mathbf{u}_j}. \tag{12}$$

A modified mass matrix $\mathbf{M}_r$ is then introduced, in which the contribution corresponding the mass of the resonant mode has been removed,

$$\mathbf{M}_r = \mathbf{M} - \frac{(\mathbf{M}\mathbf{u}_r)(\mathbf{u}_r^T \mathbf{M})}{\mathbf{u}_r^T \mathbf{M}\mathbf{u}_r} = \sum_{j \neq r} \frac{(\mathbf{M}\mathbf{u}_j)(\mathbf{u}_j^T \mathbf{M})}{\mathbf{u}_j^T \mathbf{M}\mathbf{u}_j}. \tag{13}$$

6

This mass matrix is used to define a 'frequency shifted' stiffness matrix

$$\mathbf{K}_r \;=\; \mathbf{K} \,-\, \omega_r^2 \mathbf{M}_r, \tag{14}$$

in which the resonant mode is left unaffected by the frequency shift. The eigenvector expansion of the inverse of this matrix is

$$\mathbf{K}_r^{-1} \;=\; \frac{\mathbf{u}_r \mathbf{u}_r^T}{\mathbf{u}_r^T \mathbf{K} \mathbf{u}_r} \,+\, \sum_{j \neq r} \frac{\omega_j^2}{\omega_j^2 - \omega_r^2} \frac{\mathbf{u}_j \mathbf{u}_j^T}{\mathbf{u}_j^T \mathbf{K} \mathbf{u}_j}, \tag{15}$$

in which the term corresponding to the resonant frequency $\omega_r$ is left as in the expansion of the inverse stiffness matrix, while the remaining terms are corrected corresponding to the frequency shift.

It now follows from direct multiplication, using the eigenvector expansions (12) and (15) and orthogonality of the eigenvectors, that

$$\mathbf{K}_r^{-1} \mathbf{K} \, \mathbf{K}_r^{-1} \;=\; \frac{\mathbf{u}_r \mathbf{u}_r^T}{\mathbf{u}_r^T \mathbf{K} \mathbf{u}_r} \,+\, \sum_{j \neq r} \frac{\omega_j^4}{(\omega_j^2 - \omega_r^2)^2} \frac{\mathbf{u}_j \mathbf{u}_j^T}{\mathbf{u}_j^T \mathbf{K} \mathbf{u}_j} \,, \tag{16}$$

Pre- and post-multiplication of this relation with $\mathbf{w}^T$ and $\mathbf{w}$, respectively, then leads to the following expression for the background flexibility

$$\frac{1}{k_r'} \;=\; \sum_{j \neq r} \frac{\omega_j^4}{(\omega_j^2 - \omega_r^2)^2} \frac{1}{k_j} \;=\; (\mathbf{w}^T \mathbf{K}_r^{-1}) \mathbf{K} \, (\mathbf{K}_r^{-1} \mathbf{w}) \,-\, \frac{1}{k_r}, \tag{17}$$

where $1/k_r$ is the modal flexibility of the resonant mode given by (7). The background inertia term follows in a similar way from the modified mass matrix $\mathbf{M}_r$ by forming the product

$$\mathbf{K}_r^{-1} \mathbf{M}_r \, \mathbf{K}_r^{-1} \;=\; \sum_{j \neq r} \frac{\omega_j^2}{(\omega_j^2 - \omega_r^2)^2} \frac{\mathbf{u}_j \mathbf{u}_j^T}{\mathbf{u}_j^T \mathbf{K} \mathbf{u}_j} \,, \tag{18}$$

where a factor $\omega_j^2$ has been eliminated, when substituting $\mathbf{K} \mathbf{u}_j = \omega_j^2 \mathbf{M} \mathbf{u}_j$ in the expansion (12). Pre- and post-multiplication of this relation with $\mathbf{w}^T$ and $\mathbf{w}$, respectively, then leads to the following expression for the background inertia

$$\frac{1}{\omega_r^2 m_r'} \;=\; \sum_{j \neq r} \frac{\omega_j^2 \omega_r^2}{(\omega_j^2 - \omega_r^2)^2} \frac{1}{k_j} \;=\; \omega_r^2 (\mathbf{w}^T \mathbf{K}_r^{-1}) \mathbf{M}_r \, (\mathbf{K}_r^{-1} \mathbf{w}). \tag{19}$$

The similarity between the expressions for the background coefficients $k_r'$ and $m_r'$ is noted.

The background flexibility and inertia coefficients can be evaluated without matrix inversion by the following procedure. First the modified mass matrix $\mathbf{M}_r$ and the modified stiffness matrix $\mathbf{K}_r$ are evaluated from the first expression in (13) and from (14), respectively. Then the vector $\tilde{\mathbf{u}} = \mathbf{K}_r^{-1} \mathbf{w}$ is found by solving the equation

$$\mathbf{K}_r \tilde{\mathbf{u}} \;=\; \mathbf{w}. \tag{20}$$

7

In terms of this displacement vector the background flexibility and mass coefficients take the simple form

$$\frac{1}{k'_r} + \frac{1}{k_r} = \tilde{\mathbf{u}}^T \mathbf{K} \, \tilde{\mathbf{u}} \,, \qquad \frac{1}{m'_r} = \omega_r^4 \, \tilde{\mathbf{u}}^T \mathbf{M}_r \, \tilde{\mathbf{u}} \tag{21}$$

It is clear from the expression (20) that $\tilde{\mathbf{u}}$ is the displacement vector corresponding to a normalized force $\mathbf{w}$, acting on a modified system with stiffness matrix $\mathbf{K}_r$.

The classic case of quasi-static background flexibility without inertia effects follow from setting $\omega = 0$ in the summation of the non-resonant terms in (6), whereby the corresponding background flexibility $1/k_r^0$ is found as

$$\frac{1}{k_r^0} + \frac{1}{k_r} = \mathbf{w}^T \mathbf{K}^{-1} \mathbf{w} \,. \tag{22}$$

Clearly, the product of the last two factors can be evaluated by solving a corresponding equation system, thereby avoiding the need for a matrix inversion. The quasi-static background flexibility $1/k_r^0$ is the sum of the non-resonant modal flexibilities, and therefore positive. Quasi-static background flexibility is typically used to represent higher modes in a truncated modal analysis, in which only the lower modes are retained as dynamic, [26, 27].

*2.3. Characteristic equation of structure with device*

The device frequency properties are given by a relation between the displacement $u_d$ over the device and the corresponding force $f_d = -f$,

$$u_d = H'_d(\omega) \, f_d \,, \tag{23}$$

where $H'_d(\omega)$ is the frequency response function of the device. When the device is mounted on the structure the device displacement $u_d$ equals the structure displacement $u$. Substitution of the device displacement $u_d$ from (23) and the structure displacement $u_s$ from (9) then gives the characteristic equation

$$\underbrace{\frac{\omega_r^2}{\omega_r^2 - \omega^2} \frac{1}{k_r} + \frac{1}{k'_r} - \frac{1}{m'_r} \frac{1}{\omega^2}}_{\text{structure with background terms}} + \underbrace{H'_d(\omega)}_{\text{absorber}} = 0 \,. \tag{24}$$

The solution of this equation provides the damped natural frequencies of the combined structure/absorber system, and imposing desired properties on the complex frequencies in turn determines desirable absorber parameters.

In the following three resonant absorber configurations containing the three components stiffness, damping and inertia are analyzed and calibrated. The calibration procedure is derived in two steps. The first step considers an equivalent device with frequency response function $H_d(\omega)$ mounted on a single-mode system, corresponding to the characteristic equation

$$\underbrace{\frac{\omega_r^2}{\omega_r^2 - \omega^2} \frac{1}{k_r}}_{\text{modal response}} + \underbrace{H_d(\omega)}_{\substack{\text{equivalent} \\ \text{absorber}}} = 0 \,. \tag{25}$$

8

This determines a set of parameters of the equivalent device.

The second step then consists in deducing the parameters of the original device from the equivalent device parameters by equating the non-resonant terms in (24) and (25), leading to the equivalence relation

$$H_d(\omega) \simeq \frac{1}{k_r'} - \frac{1}{m_r'}\frac{1}{\omega^2} + H_d'(\omega). \tag{26}$$

If the effect of the non-resonant background modes is disregarded, the first step gives the device parameters directly.

According to the adopted notation the device response function $H_d(\omega)$ corresponds to a direct calibration based on a single mode, whereas the response function $H_d'(\omega)$ corresponds to a device on a structure represented by the modal response plus the background terms with parameters $1/k_r'$ and $1/m_r'$. In the design computations the relative effect of the background flexibility and the background inertia will be represented via the non-dimensional parameters

$$\kappa_r' = \frac{k_r}{k_r'}, \qquad \mu_r' = \frac{m_r}{m_r'}, \tag{27}$$

where $m_r = k_r/\omega_r^2$ is the resonant modal mass. Note, that by the definition of the non-dimensional background parameters in terms of the reciprocals, the absence of these effects corresponds to $\kappa_r' = 0$ and $\mu_r' = 0$, respectively.

## 3. Absorber with parallel stiffness and damper elements

In the resonant inerter based absorber shown in Fig. 2 a spring and a damping element are coupled in parallel. The device parameters are the stiffness $k_d$, the equivalent inerter mass $m_d$ and the damping coefficient $c_d$. This device is analogous to the tuned mass absorber apart from the fact that the inerter based device has two points of fixture and operates on the relative motion of these points, whereas the tuned mass absorber operates on the absolute motion of a single point of fixture. The similarity of the calibration procedure for these two devices was discussed in [29]. Here the procedure is summarized in a self-contained form that permits generalization to other inerter based devices as demonstrated in the subsequent sections. The calibration of the device on an idealized structure, neglecting the influence of non-resonant modes, is presented in Section 3.1, and subsequently generalized to account for the effect of the non-resonant modes in Section 3.2.

### 3.1. Single-mode calibration

The force $f_d$ in the device can be given both in terms of the relative displacement $u_1$ over the parallel stiffness and damper elements and in terms of the displacement $u_2$ over the inerter element,

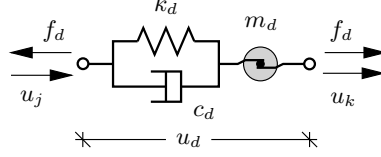$$f_d = (k_d + i\omega c_d)u_1 = -\omega^2 m_d\, u_2. \tag{28}$$

Figure 2: Resonant absorber with parallel spring and damper.

This gives the total displacement over the device $u_d = u_1 + u_2$ as

$$u_d = \left( \frac{1}{k_d + i\omega c_d} - \frac{1}{\omega^2 m_d} \right) f_d = H_d(\omega) f_d. \tag{29}$$

In the following it is convenient to introduce the undamped natural frequency $\omega_d$ of the device with locked points of fixture and the corresponding device damping ratio $\zeta_d$ by the relations

$$\omega_d^2 = \frac{k_d}{m_d}, \qquad \zeta_d = \frac{c_d}{2\sqrt{k_d m_d}}. \tag{30}$$

The size of the device is defined via the mass ratio

$$\mu = \frac{m_d}{m_r}, \tag{31}$$

giving the equivalent inerter mass relative to the resonant modal mass $m_r = k_r/\omega_r^2$.

When inserting the device frequency response function $H_d(\omega)$ from (29) into (25), the following characteristic equation is found,

$$\omega^4 - \left[ (1+\mu)\omega_d^2 + \omega_r^2 \right]\omega^2 + \omega_r^2\omega_d^2 - 2i\zeta_d\omega\omega_d\left[ (1+\mu)\omega^2 - \omega_r^2 \right] = 0. \tag{32}$$

This equation is completely analogous to the characteristic equation for a tuned mass damper on an idealized single-mass structure, apart from the fact that the present equation refers to the relative motion of two points on the structure as reflected by the two entries in the integer array $\mathbf{w}$ used to define the scalar representation of the structure in (5)–(7). The design, prescribing an optimal combination of device parameters, can be obtained by a simple pole placement procedure [7, 28], which for the present device reproduces the classic frequency tuning of the tuned mass damper, [1]. The advantage of the present form of pole placement procedure is that the parameters can be identified directly from the coefficients of the characteristic equation for a family of inerter based devices.

First a reference frequency $\omega_0$ is introduced such that the constant term is $\omega_0^4$. This gives

$$\omega_0^2 = \omega_r\omega_d. \tag{33}$$

Then the coefficients of the linear and the cubic term are balanced such that the ratio of their coefficients is $\omega_0^2$. For device damping ratio $\zeta_d$ below a certain limit this leads to natural frequencies of the two modes that are inverse points in the circle $|\omega| = \omega_0$,
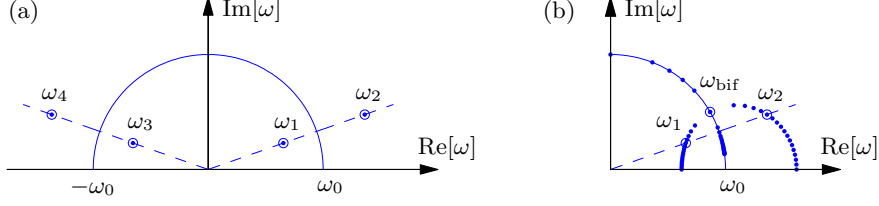
Figure 3: (a) Complex roots $\omega_1, \omega_2$ and $\omega_3, \omega_4$ as inverse points of circle $|\omega| = \omega_0$, (b) Root-locus diagram with bifurcation point $\omega_{\text{bif}}$.

corresponding to $\omega_1 \bar{\omega}_2 = \omega_0^2$, illustrated in Fig. 3. Frequencies represented by inverse points correspond to equal damping ratio, whereby

$$\omega_{1,2} \;=\; |\omega_{1,2}|\big(\sqrt{1-\zeta^2} + i\zeta\big). \tag{34}$$

Balancing the coefficients of the linear and cubic terms gives the relation

$$\omega_0^2 \;=\; \frac{\omega_r^2}{1+\mu}, \tag{35}$$

and combination with the relation (33) then leads to the device frequency

$$\omega_d \;=\; \frac{\omega_r}{1+\mu}, \tag{36}$$

whereby the device frequency $\omega_d$ is tuned below the resonant modal frequency $\omega_r$. This result leads to the device stiffness ratio

$$\kappa \;=\; \frac{k_d}{k_r} \;=\; \Big(\frac{\omega_d}{\omega_r}\Big)^2 \mu \;=\; \frac{\mu}{(1+\mu)^2}, \tag{37}$$

where the denominator is due to the frequency tuning, and implies that $\kappa < \mu$.

With the device frequency (36) the characteristic equation (32) takes a simplified form in terms of the reference frequency $\omega_0$,

$$\omega^4 \;-\; (2+\mu)\omega_0^2\omega^2 \;+\; \omega_0^4 \;-\; 2i\zeta_d\sqrt{1+\mu}\,\omega_0\omega(\omega^2 - \omega_0^2) \;=\; 0\,. \tag{38}$$

After division by $\omega_0^2\omega^2$ the equation can be recast in the following quadratic format

$$\Big(\frac{\omega}{\omega_0} - \frac{\omega_0}{\omega}\Big)^2 \;-\; 2i\zeta_d\sqrt{1+\mu}\Big(\frac{\omega}{\omega_0} - \frac{\omega_0}{\omega}\Big) \;-\; \mu \;=\; 0\,. \tag{39}$$

that permits a direct solution as well as a detailed analysis of the root-locus curve, [7]. Note, that this quadratic format is a direct consequence of adjusting the balance between the linear and cubic terms in the characteristic equation such that they contain the factor $\omega\omega_0(\omega^2 - \omega_0^2)$. This is a general procedure for determining the device frequency $\omega_d$ that also applies to different resonant absorber configurations as discussed later.

11

At zero damping the frequencies $\omega_1$ and $\omega_2$ are located at the positive real axis. When increasing the damping the frequencies move up into the imaginary part of the plane along curves that correspond closely to a semi-circle for a mass ratio $\mu \lesssim 0.1$, well within the magnitude encountered in most practical applications. The equation (39) is quadratic in the combined term in the parentheses. A bifurcation is encountered when the damping ratio leads to a double root of this equation at $\zeta_{\mathrm{bif}}^2 = \mu/(1+\mu)$. The device damping ratio essentially acts as an arc-length parameter on the semi-circle in the complex point with the bifurcation value marking the top point. The calibration value should reflect a balance between zero damping at the real axis and a double root at the bifurcation point. It was found in [7] that an optimal balance corresponds to roots located about $45°$ up the semicircle from the real axis, whereby

$$\zeta_d^2 \;=\; \frac{\zeta_{\mathrm{bif}}^2}{2} \;=\; \frac{1}{2}\frac{\mu}{1+\mu}. \tag{40}$$

This value is slightly larger than the classic value for the tuned mass damper with coefficient $3/8$, [1, 2], but gives a more flat plateau of the response as well as minimum local amplitude of the device as illustrated in Fig. 4, showing the structural amplification and the device response for the classic damping with factor $3/8$, for the present 'optimal' damping with factor $1/2$, and for bifurcation damping with factor $1$.
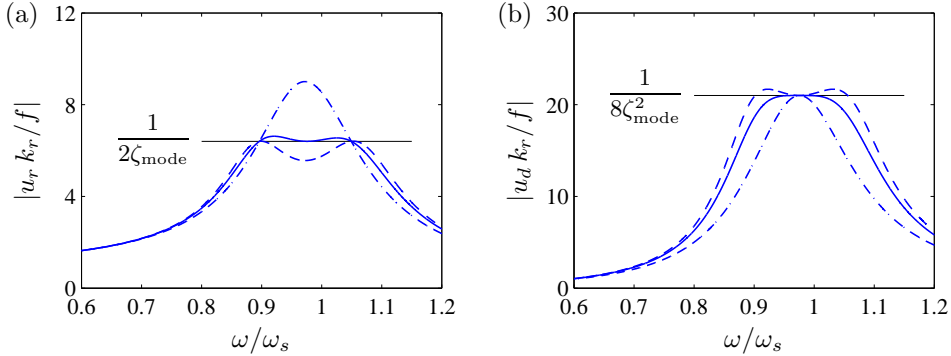


Figure 4: Dynamic amplification for $\mu = 0.05$. (a) structure motion $u_r$ and (b) relative device motion $u_d$. Damping parameter: - - $\zeta_{\mathrm{classic}}$, — $\zeta_{\mathrm{opt}}$, - · - $\zeta_{\mathrm{bif}}$.

The typical single-mode design procedure is outlined in Table 1 for both the present device with parallel spring–damper elements as well as for the alternative configuration of parallel inerter–damper described in section 4.1. A very simple and direct design procedure follows from the parameter expressions derived above together with the structural amplification illustrated in Fig. 4. It follows from the complex root locus analysis that the device damping ratio contributes $\frac{1}{2}\zeta_d$ to the damping of each of the modes, in which the resonant absorber splits the original resonant mode, [7, 28]. Furthermore, these modes typically retain the original structural damping $\zeta_{\mathrm{struc}}$, [28, 29], whereby the representative resulting damping ratio of these modes is determined by

$$\zeta_{\mathrm{mode}} \;\simeq\; \zeta_{\mathrm{struc}} + \tfrac{1}{2}\zeta_d \tag{41}$$

12

Table 1: Single-mode design procedure for single damper devices.

|  | Parallel stiffness-damper | Parallel inerter-damper |
|---|---|---|
| Modal damping: | $2\zeta_{\mathrm{mode}} = \dfrac{1}{DAF}$ | |
| Device damping: | $\zeta_d = 2(\zeta_{\mathrm{mode}} - \zeta_{\mathrm{struc}})$ | |
| Mass/stifness ratio: | $\mu = \dfrac{2\zeta_d^2}{1 - 2\zeta_d^2}$ <br> $\kappa = \dfrac{\mu}{(1+\mu)^2}$ | $\kappa = \dfrac{2\zeta_d^2}{1 - 2\zeta_d^2}$ <br> $\mu = \dfrac{\kappa}{(1+\kappa)^2}$ |
| Device parameters: | $m_d = \mu\,m_r,\ \ k_d = \kappa\,k_r,\ \ c_d = 2\zeta_d\sqrt{m_d k_d}$ | |

This modal damping ratio is closely related to the modal amplification as illustrated in Fig. 4, showing that the dynamic amplification factor is closely represented by $DAF = 1/2\zeta_{\mathrm{mode}}$. Thus, a typical first step in the design of the device is to determine the modal damping ratio including the effect of the device from the design value of the dynamic amplification factor. This is the first step shown in Table 1. The second step is to calculate the device damping ratio from (41). For the parallel spring–damper device the mass ratio then follows from (40). The stiffness ratio is then given by (37), and the actual parameters are evaluated from the non-dimensional parameters as shown in the table. This procedure applies to an idealized structure, represented by a concentrated mass. In most applications of inerter based devices the relative motion of the two points of attachment of the device also depends on deformation associated with the non-resonant background modes, and thus a full design also includes evaluation of the effect of this contribution as described in the next section.

### 3.2. Accounting for background deformation

The effect of background flexibility and inertia is included in the design of the device by an equivalence between the response relation (24) in terms of the actual device frequency function $H_d'(\omega)$ with parameters $k_d'$, $m_d'$ and $c_d'$ and the background stiffness $k_r'$ and mass $m_r'$, and the idealized single-mode response relation (25) in terms of the equivalent device frequency function $H_d(\omega)$ with parameters $k_d$, $m_d$ and $c_d$. The present task is to determine optimal parameters $k_d'$, $m_d'$ and $c_d'$ in the frequency response function $H_d'(\omega)$. The background correction terms are therefore moved to the other side of the equivalence relation (26), whereby

$$H_d'(\omega) \simeq H_d(\omega) - \frac{1}{k_r'} + \frac{1}{\omega^2}\frac{1}{m_r'}. \tag{42}$$

The particular format (29) for the parallel spring-damper configuration then gives the equation

$$\frac{1}{k_d' + i\omega c_d'} - \frac{1}{\omega^2 m_d'} \simeq \left(\frac{1}{k_d + i\omega c_d} - \frac{1}{k_r'}\right) - \frac{1}{\omega^2}\left(\frac{1}{m_d} - \frac{1}{m_r'}\right). \tag{43}$$

13

Table 2: Background mode correction for basic three-component devices.

| | Parallel stiffness-damper | Parallel inerter-damper |
|---|---|---|
| Background parameters: | $\kappa'_r = \dfrac{k_r}{k'_r}$ , $\mu'_r = \dfrac{m_r}{m'_r}$ | |
| Device stiffness: | $k'_d = \dfrac{k_d}{1 - \kappa'_r \kappa}$ | |
| Device mass: | $m'_d = \dfrac{m_d}{1 - \mu'_r \mu}$ | |
| Device damping: | $c'_d = \dfrac{c_d}{(1 - \kappa'_r \kappa)^2}$ | $c'_d = \dfrac{c_d}{(1 - \mu'_r \mu)^2}$ |

The device mass $m'_d$ follows directly from the second term on the right side as

$$m'_d = \frac{m'_r m_d}{m'_r - m_d}. \tag{44}$$

Division by the equivalent background mass $m'_r$ then gives the result in the form

$$m'_d = \frac{m_d}{1 - \mu'_r \mu}, \tag{45}$$

where $\mu$ is the single-mode design mass ratio and $\mu'_r$ is the background mass coefficient defined in (27b) as $\mu'_r = m_r/m'_r$. The formula provides a correction to the device mass $m_d$ obtained by single-mode calibration. It is seen that the device mass $m'_d$ determined by including the effect of the background modes is larger than $m_d$ determined from the classic single-mode design. In spite of a theoretical singularity of the background mode correction in (45) a mass ratio used in practice will usually lead to results well removed from this singularity.

The design values of the device stiffness $k'_d$ and damping $c'_d$, when accounting for the background modes, are now found from the remaining terms in the equivalence relation (43),

$$k'_d + i\omega c'_d \simeq \frac{(k_d + i\omega c_d)k'_r}{k'_r - (k_d + i\omega c_d)} \tag{46}$$

The right hand side is reduced to real and imaginary parts by multiplication with the conjugate of the denominator, whereby

$$k'_d + i\omega c'_d \simeq \frac{k_d\left(1 - \dfrac{k_d}{k'_r}\right) - \omega^2 \dfrac{c_d^2}{k'_r} + i\omega c_d}{\left(1 - \dfrac{k_d}{k'_r}\right)^2 + \omega^2\left(\dfrac{c_d}{k'_r}\right)^2} \tag{47}$$

It is easily established, see e.g. [29], that in the relevant frequency interval around resonance the terms containing $(\omega c_d)^2$ will be fairly small, and when discarding these

14

terms the following design parameters are obtained for including background effects,

$$k'_d = \frac{k_d}{1 - \kappa'_r \kappa}, \qquad c'_d = \frac{c_d}{(1 - \kappa'_r \kappa)^2}, \qquad (48)$$

where $\kappa$ is the single-mode design stiffness ratio and $\kappa'_r$ is the background mass coefficient defined in (27a) as $\kappa'_r = k_r/k'_r$. It is seen that including the effect of the background modes leads to larger design values of both device stiffness and device damping. In practice, the device has much less mass than the structure and thus $\mu \ll 1$, whereby $\kappa \ll 1$. Thus, even a rather large background stiffness coefficient $\kappa'_r$ will generally lead to representative values of $k'_d$ and $c'_d$ in spite of the theoretical singularity of the background correction formulae (48). The correction of device parameters for flexibility and inertia of background modes of the device with parallel stiffness and damper elements is shown in the left side of Table 2. It is noted that for the present device the background correction of the damping coefficient is given in terms of the device and background stiffness parameters.

## 4. Absorber with parallel inerter and damper elements

An alternative form of a resonant inerter based vibration absorber device is shown in Fig. 5. In this device the damper is in parallel with the inerter, and thus the important phase change in the spring force of the previous device is now changed to a phase change of the force component in the inerter. The device has two points of fixture, and thus reacts ~~to relative motion~~ of these points.
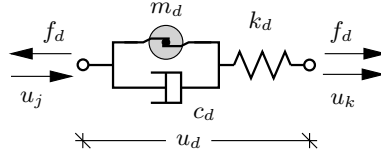


Figure 5: Resonant absorber with parallel inerter and damper.

### 4.1. Single-mode calibration

For the device in Fig. 5 the device force $f_d$ can be expressed either as the relative displacement $u_1$ over the spring or the relative displacement $u_2$ over the parallel inerter and damper elements,

$$f_d = k_d u_1 = (i\omega c_d - \omega^2 m_d)u_2. \qquad (49)$$

This gives the total displacement over the device $u_d = u_1 + u_2$ as

$$u_d = \left( \frac{1}{k_d} + \frac{1}{i\omega c_d - \omega^2 m_d} \right) f_d = H_d(\omega) f. \qquad (50)$$

The natural frequency of the undamped device $\omega_d$ and the inerter damping ratio $\zeta_d$ are given by (30). For the present device the mass ratio $\mu$ given in (31) is supplemented by the stiffness ratio

$$\kappa = \frac{k_d}{k_r},\qquad(51)$$

giving the device stiffness relative to the resonant modal stiffness. In terms of these parameters the characteristic equation of (25) takes the form

$$\omega^4 - \left[\omega_d^2 + (1+\kappa)\omega_r^2\right]\omega^2 + \omega_r^2\omega_d^2 - 2i\zeta_d\omega\omega_d\left[\omega^2 - (1+\kappa)\omega_r^2\right] = 0\,.\qquad(52)$$

It is noted that this equation looks rather similar to the characteristic equation (32) for the previous device.

The design parameters can now be determined by the procedure described in Section 3.1. The reference frequency $\omega_0$ defined by the constant term is given by (33) also in the present case. Balancing the ratio of the coefficients of the linear and the cubic terms to obtain equal modal damping takes the form

$$\omega_0^2 = (1+\kappa)\omega_r^2,\qquad(53)$$

and combination with the relation (33) then leads to the device frequency

$$\omega_d = (1+\kappa)\omega_r,\qquad(54)$$

whereby the present device frequency $\omega_d$ is tuned above the resonant modal frequency $\omega_r$. This result leads to the device mass ratio

$$\mu = \frac{m_d}{m_r} = \left(\frac{\omega_r}{\omega_d}\right)^2 \kappa = \frac{\kappa}{(1+\kappa)^2},\qquad(55)$$

where the denominator is due to the frequency tuning, and $\mu < \kappa$.

With the device frequency (54) the present characteristic equation (52) takes a simplified form in terms of the reference frequency $\omega_0$,

$$\omega^4 - (2+\kappa)\omega_0^2\omega^2 + \omega_0^2 - 2i\zeta_d\sqrt{1+\kappa}\,\omega_0\omega(\omega^2 - \omega_0^2) = 0\,.\qquad(56)$$

It is observed that this characteristic equation becomes identical to the characteristic equation (38) for the parallel spring–damper device, when the mass ratio $\mu$ is replaced by the stiffness ratio $\kappa$. This implies that the root locus analysis can be transferred directly when substituting the stiffness ratio $\kappa$ for the mass ratio $\mu$ in the previous analysis/argument. Thus, in the present case the bifurcation point is attained for a device damping ratio where $\zeta_{\text{bif}}^2 = \kappa/(1+\kappa)$, and the appropriate balanced design is attained for the device damping ratio

$$\zeta_d^2 = \frac{\zeta_{\text{bif}}^2}{2} = \frac{1}{2}\frac{\kappa}{1+\kappa}\,.\qquad(57)$$

It is seen that this formula is similar to (40) for the parallel stiffness–inerter device. In fact, the design procedures of the two devices, shown in Table 1 are identical, apart from interchange of the roles of mass and stiffness ratio parameters $\mu$ and $\kappa$.

16

### 4.2. Accounting for background deformation

The principle of the correction for background modes is the same as for the previous device, and thus the actual device frequency response function $H'(\omega)$ is determined by introducing the device response format (50) into the equivalence relation (42), whereby

$$\frac{1}{k'_d} - \frac{1}{\omega^2 m'_d - i\omega c'_d} = \Big(\frac{1}{k_d} - \frac{1}{k'_r}\Big) - \Big(\frac{1}{\omega^2 m_d - i\omega c_d} - \frac{1}{\omega^2 m'_r}\Big). \qquad (58)$$

For this device the equivalence relation (58) determines the device stiffness $k'_r$ from the first term on the right side as

$$k'_d = \frac{k'_r \, k_d}{k'_r - k_d}. \qquad (59)$$

Division by the equivalent background stiffness $k'_r$ then gives the device stiffness modification due to background effects in the compact form

$$k'_d = \frac{k_d}{1 - \kappa'_r \, \kappa}, \qquad (60)$$

where $\kappa$ is the single-mode design stiffness ratio and $\kappa'_r$ is the background flexibility coefficient defined in (27a) as $\kappa'_r = k_r/k'_r$. Note the complete similarity between the modification of the device stiffness for the present parallel inerter-damper device and the relation (63) for the modification of the device mass in the case of the parallel stiffness-damper device.

The design values of the device mass $m'_d$ and the damping $c'_d$ are determined from the remaining part of the equivalence equation (58), whereby

$$\omega^2 m'_d - i\omega c'_d = \frac{(\omega^2 m_d - i\omega c_d)\,\omega^2 m'_r}{\omega^2 m'_r - (\omega^2 m_d - i\omega c_d)} \qquad (61)$$

The right hand side is reduced to real and imaginary parts by multiplication with the conjugate of the denominator, whereby

$$m'_d - \frac{i}{\omega}c'_d = \frac{m_d\Big(1 - \dfrac{m_d}{m'_r}\Big) - \dfrac{c_d^2}{\omega^2 m'_r} - \dfrac{i}{\omega}c_d}{\Big(1 - \dfrac{m_d}{m'_r}\Big)^2 + \Big(\dfrac{c_d}{\omega m'_r}\Big)^2}. \qquad (62)$$

Also in this case the terms containing $c_d^2/\omega^2$ will be fairly small in the resonance frequency interval. When discarding these terms the following design parameters are obtained for including background effects,

$$m'_d = \frac{m_d}{1 - \mu'_r \, \mu}, \qquad c'_d = \frac{c_d}{(1 - \mu'_r \, \mu)^2}, \qquad (63)$$

where $\mu$ is the single-mode design mass ratio and $\mu'_r$ is the background mass coefficient defined in (27b) as $\mu'_r = m_r/m'_r$. As for the previous device including the background modes increases the design mass and damping. The correction of device parameters

for flexibility and inertia of background modes of the device with parallel inerter and damper elements is shown in the right side of Table 2.

It is observed that for the present and the previous device the design mass is increased by the factor $(1 - \mu'_r \mu)^{-1}$ as function of single mode mass ratio and the background mass coefficient, while the design stiffness is increased by a similar factor $(1 - \kappa'_r \kappa)^{-1}$ in terms of the single mode stiffness ratio and the background flexibility coefficient. In contrast, the damper coefficient is modified by the square of the stiffness coefficient, when acting in parallel with the spring, and by the square of the mass coefficient when acting in parallel with the inerter.

## 5. Absorber with dampers in parallel with inerter and stiffness elements

In the two resonant inerter based vibration absorbers analyzed in the previous sections a single damper was placed in parallel with a spring or the inerter, respectively. As demonstrated that leads to tuning of the device frequency $\omega_d$ below or above the original resonant frequency $\omega_r$ of the structure. Figure 6 shows a device with identical dampers $c_{dk} = c_{dm}$ in parallel with the spring and the inerter, respectively. It is now demonstrated that this combined device leads to an optimal tuning frequency $\omega_d$ that is identical to the original structure resonant frequency $\omega_r$. Hereby the mass ratio $\mu$ and stiffness ratio $\kappa$ also become identical.
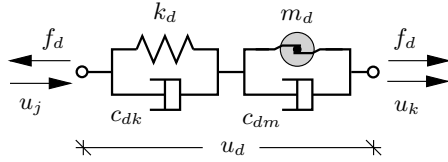


Figure 6: Resonant absorber with identical dampers in parallel with spring and inerter elements.

*5.1. Single-mode calibration*

The force $f_d$ in the device can be given both in terms of the relative displacement $u_1$ over the parallel stiffness and damper elements and in terms of the displacement $u_2$ over the inerter element and damper element,

$$f_d = (k_d + i\omega c_{dk})u_1 = (-\omega^2 m_d + i\omega c_{dm})u_2. \tag{64}$$

The total displacement over the device $u_d = u_1 + u_2$ then follows as

$$u_d = \left( \frac{1}{k_d + i\omega c_{dk}} - \frac{1}{\omega^2 m_d - i\omega c_{dm}} \right) f_d = H_d(\omega) f_d. \tag{65}$$

The undamped device frequency is given as before by (30a), and the device damping ratio is defined to describe the effect of both dampers $c_d = c_{dk} + c_{dm}$,

$$\zeta_d = \frac{c_d}{2\sqrt{k_d m_d}}. \tag{66}$$

18

The size of the device is here defined via the mass ratio

$$\mu = \frac{m_d}{m_r}, \tag{67}$$

giving the equivalent inerter mass relative to the resonant modal mass $m_r$.

When inserting the device frequency response function $H_d(\omega)$ from (65) into (25), the following characteristic equation is found,

$$\omega^4 - \left[\omega_r^2 + \left((1+\mu(1+\zeta_d^2))\omega_d^2\right]\omega^2 + \omega_r^2\omega_d^2 + i\zeta_d\omega_d\omega\left[2\omega_r^2 + \mu\omega_d^2 - (2+\mu)\omega^2\right] = 0. \tag{68}$$

As before, a reference frequency $\omega_0$ is introduced such that the constant term is $\omega_0^4$. This gives

$$\omega_0^2 = \omega_r\omega_d. \tag{69}$$

Now, the coefficients of the linear and the cubic term are balanced such that the ratio of their coefficients is $\omega_0^2$, whereby

$$2\omega_r^2 + \mu\omega_d^2 = (2+\mu)\omega_0^2 = (2+\mu)\omega_r\omega_d. \tag{70}$$

Balancing the coefficients of the linear and cubic terms gives the relation

$$\omega_d = \omega_r = \omega_0. \tag{71}$$

Thus, the optimal frequency tuning of the present double-damper device is at the resonant frequency. It is seen that this frequency tuning determines the device stiffness ratio as

$$\kappa = \frac{k_d}{k_r} = \left(\frac{\omega_d}{\omega_r}\right)^2\mu = \mu, \tag{72}$$

and thus the device mass ratio and stiffness ratio are equal for the optimally tuned double-damper device.

With the device frequency tuning given by (71) the characteristic equation (68) takes a simplified form, here given in terms of the reference frequency $\omega_0$,

$$\omega^4 - \left(2 + \mu(1+\zeta_d^2)\right)\omega_0^2\omega^2 + \omega_0^4 + 2i\zeta_d(1+\tfrac{1}{2}\mu)\,\omega_0\omega(\omega^2 - \omega_0^2) = 0. \tag{73}$$

This equation is similar but not identical to the two previous expressions (39) and (56) for the reduced characteristic equation. In order to identify the damping ratio $\zeta_{\text{bif}}$, corresponding to the bifurcation point in the root locus graph, the equation is divided by $\omega_0^2\omega^2$, leading to the quadratic format

$$\left(\frac{\omega}{\omega_0} - \frac{\omega_0}{\omega}\right)^2 - 2i\zeta_d(1+\tfrac{1}{2}\mu)\left(\frac{\omega}{\omega_0} - \frac{\omega_0}{\omega}\right) - \mu(1+\zeta_d^2) = 0. \tag{74}$$

The bifurcation point corresponds to a double root, identified by vanishing of the discriminant,

$$\left[\zeta_{\text{bif}}(1+\tfrac{1}{2}\mu)\right]^2 = \mu(1+\zeta_{\text{bif}}^2). \tag{75}$$

This equation determines the bifurcation value of the device damping ratio as

$$\zeta_{\text{bif}}^2 = \frac{\mu}{1 + (\mu/2)^2} \simeq \mu. \tag{76}$$

19

Table 3: Single-mode design procedure for double damper device.

| | Dampers in parallel with both stiffness and inerter |
|---|---|
| Modal damping: | $2\zeta_{\text{mode}} = \dfrac{1}{DAF}$ |
| Device damping: | $\zeta_d = 2(\zeta_{\text{mode}} - \zeta_{\text{struc}})$ |
| Mass/stifness ratio: | $\mu = \kappa = 2\zeta_d^2$ |
| Device parameters: | $m_d = \mu m_r, \quad k_d = \kappa k_r, \quad c_d = c_{dk} + c_{dm} = 2\zeta_d\sqrt{m_d k_d}$ |

The last approximation follows from the observation that the mass ratio is most often in the order of a few percent. The root locus curve corresponding to the characteristic equation (73) is identical to those of the two other resonant devices apart from a slightly different parametrization. Also in this case the device damping ratio $\zeta_d$ acts as an arc length parameter on the initial part of the root locus curve, leading to the design value

$$\zeta_d^2 = \frac{\zeta_{\text{bif}}^2}{2} = \frac{\mu/2}{1 + (\mu/2)^2} \simeq \frac{\mu}{2}, \tag{77}$$

slightly larger than for the two other resonant absorbers. The design procedure for the double-damper device on an idealized structure is summarized in Table 3.

### 5.2. Accounting for background deformation

As in the previous two cases the background effects are included in the design by assuming that the actual device frequency response function $H'(\omega)$, when combined with the background flexibility and inertia, provides a close approximation to the ideal device frequency response function $H(\omega)$ determined above. When using the device frequency response format defined by (65) in the equivalence relation (42), this gives

$$\frac{1}{k_d' + i\omega c_{dk}'} - \frac{1}{\omega^2 m_d' - i\omega c_{dm}'} \simeq \left(\frac{1}{k_d + i\omega c_{dk}} - \frac{1}{k_r'}\right) - \left(\frac{1}{\omega^2 m_d - i\omega c_{dm}} - \frac{1}{\omega^2 m_r'}\right). \tag{78}$$

where the two damping parameters $c_{dk} = c_{dm} = c_d/2$ have been used for clarity. The stiffness and mass relations are obtained from the coefficients to $\omega^0$ and $\omega^{-2}$ in the limit of no damping, whereby

$$\frac{1}{k_d'} = \frac{1}{k_d} - \frac{1}{k_r'}, \qquad \frac{1}{m_d'} = \frac{1}{m_d} - \frac{1}{m_r'}. \tag{79}$$

When introducing the background flexibility and inertia factors $\kappa_r' = k_r/k_r'$ and $\mu_r' = m_r/m_r'$, the actual parameters are determined as

$$k_d' = \frac{k_d}{1 - \kappa_r'\kappa}, \qquad m_d' = \frac{m_d}{1 - \mu_r'\mu}. \tag{80}$$

20

Table 4: Background mode correction for double damper device.

| | Dampers in parallel with both stiffness and inerter |
|---|---|
| Background parameters: | $\kappa_r' = \dfrac{k_r}{k_r'} \, , \quad \mu_r' = \dfrac{m_r}{m_r'}$ |
| Device stiffness: | $k_d' = \dfrac{k_d}{1 - \kappa_r' \kappa}$ |
| Device mass: | $m_d' = \dfrac{m_d}{1 - \mu_r' \mu}$ |
| Device damping: | $c_d' = \left( \dfrac{1}{(1 - \kappa_r' \kappa)^2} + \dfrac{1}{(1 - \mu_r' \mu)^2} \right) \dfrac{c_d}{2}$ |

The background correction of these parameters is seen to be identical to that in the two other resonant devices.

The background correction of the damping parameters is determined from the first term of a Taylor expansion of the real part, giving

$$\frac{\omega\, c_{dk}'}{(k_d')^2} + \frac{\omega\, c_{dm}'}{(\omega^2 m_d')^2} \simeq \frac{\omega\, c_{dk}}{(k_d)^2} + \frac{\omega\, c_{dm}}{(\omega^2 m_d)^2}. \tag{81}$$

When removing the common factor $\omega$ and multiplying the equation by $(k_d')^2$ the following form is obtained

$$c_{dk}' + \left( \frac{k_d'}{\omega^2 m_d'} \right)^2 c_{dm}' \simeq \left( \frac{k_d'}{k_d} \right)^2 c_{dk} + \left( \frac{k_d'}{\omega^2 m_d} \right)^2 c_{dm}. \tag{82}$$

The frequency of the actual device is determined as $(\omega_d')^2 = k_d'/m_d'$. When the equation is satisfied at this frequency, the following simplified form is obtained

$$c_{dk}' + c_{dm}' = \left( \frac{k_d'}{k_d} \right)^2 c_{dk} + \left( \frac{m_d'}{m_d} \right)^2 c_{dm}. \tag{83}$$

The background correction of the damping is found from substitution of the stiffness and mass correction factors (80) into this equation. In the ideal device the damping constants were taken to be equal, $c_{dk} = c_{dm} = c_d/2$. For practical design purposes a similar condition is imposed on the actual damping parameters, $c_{dk}' = c_{dm}' = c_d'/2$, whereby the background correction of the damping parameter(s) is found as

$$c_d' = \left( \frac{1}{(1 - \kappa_r' \kappa)^2} + \frac{1}{(1 - \mu_r' \mu)^2} \right) \frac{c_d}{2}. \tag{84}$$

In the present calibration procedure the mass ratio and the stiffness ratio of the ideal device were found to be equal, $\mu = \kappa$, whereas the background inertia and flexibility coefficients $\mu_r'$ and $\kappa_r'$ are typically different.

The non-resonant background mode corrections for the double damper device are summarized in Table 4. It is seen that the correction factors on the device stiffness

and inertia are identical to those of the basic three-component device sown in Table 2, whereas the correction of the device damping coefficient $c_d$ corresponds to application of the mean value of the two factors given in Table 2.

## 6. Example

The following example illustrates the straightforward implementation of the inerter based devices in a standard finite element model and makes a brief comparison of the three devices when calibrated as described in detail in the previous sections.

### 6.1. Implementation of resonant inerter based damping devices

Let the equation of motion of the original structure without a damping device be expressed by the following standard equation of linear dynamics,

$$\mathbf{M}\ddot{\mathbf{u}} + \mathbf{C}\dot{\mathbf{u}} + \mathbf{K}\mathbf{u} = \mathbf{f}, \tag{85}$$

with mass, damping and stiffness matrices $\mathbf{M}$, $\mathbf{C}$, and $\mathbf{K}$, respectively. The displacement vector of the original structure is denoted $\mathbf{u}$ and the corresponding external load vector $\mathbf{f}$. When evaluating the performance of the resonant absorbers presented in the previous sections, it is advantageous to introduce an additional degree of freedom $u_*$, expressing e.g. the extension of the inerter element of the resonant device. The spring element and the inerter element are placed in series in each of the devices discussed here, and the extension of the spring element therefore takes the form

$$u_d - u_* = \mathbf{w}^T\mathbf{u} - u_*. \tag{86}$$

The extended displacement and load vectors to be used for the structure including the resonant device are introduced as

$$\mathbf{u}_*^T = [\mathbf{u}^T, u_*], \qquad \mathbf{f}_*^T = [\mathbf{f}^T, 0]. \tag{87}$$

The extended equation of motion then takes the form

$$\mathbf{M}_*\ddot{\mathbf{u}}_* + \mathbf{C}_*\dot{\mathbf{u}}_* + \mathbf{K}_*\mathbf{u}_* = \mathbf{f}_*, \tag{88}$$

where the extended stiffness matrix and the extended mass matrix take the form

$$\mathbf{K}_* = \begin{bmatrix} \mathbf{K} + k_d\mathbf{w}\mathbf{w}^T & -k_d\mathbf{w} \\ -k_d\mathbf{w}^T & k_d \end{bmatrix}, \qquad \mathbf{M}_* = \begin{bmatrix} \mathbf{M} & \mathbf{0} \\ \mathbf{0}^T & m_d \end{bmatrix} \tag{89}$$

for all three absorber types. The damping matrix of the type 1 absorber from Fig. 2 with the damping element in parallel with the stiffness element is augmented like the stiffness matrix, whereas the damping matrix of the type 2 absorber from Fig. 5 with the damping element in parallel with the stiffness element is augmented like the mass matrix,

$$\mathbf{C}_*^{(1)} = \begin{bmatrix} \mathbf{C} + c_d\mathbf{w}\mathbf{w}^T & -c_d\mathbf{w} \\ -c_d\mathbf{w}^T & c_d \end{bmatrix}, \qquad \mathbf{C}_*^{(2)} = \begin{bmatrix} \mathbf{C} & \mathbf{0} \\ \mathbf{0}^T & c_d \end{bmatrix} \tag{90}$$

Finally, the absorber of type 3 with two damper elements of magnitude $\frac{1}{2}c_d$ shown in Fig. 6 leads to

$$\mathbf{C}_*^{(3)} \;=\; \tfrac{1}{2}\mathbf{C}_*^{(1)} \;+\; \tfrac{1}{2}\mathbf{C}_*^{(2)} \;=\; \left[ \begin{array}{cc} \mathbf{C} + \frac{1}{2}c_d\mathbf{w}\mathbf{w}^T & -\frac{1}{2}c_d\mathbf{w} \\ -\frac{1}{2}c_d\mathbf{w}^T & c_d \end{array} \right] \tag{91}$$

With these expressions and the parameter values obtained by the calibration procedure described in the previous sections the finite element equations of the augmented system including the resonant damping device can be set up directly.

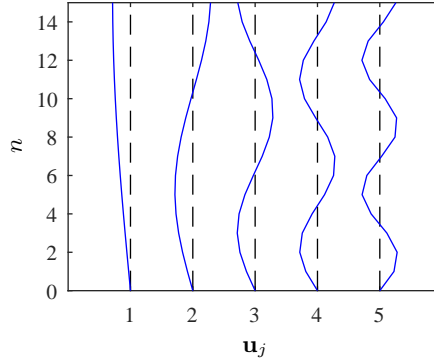### 6.2. Single vibration absorber on simple shear building



Figure 7: First five natural modes $\mathbf{u}_j$ of a 15-story shear building.

The performance and relative merits of the three resonant inerter based devices treated in this paper are illustrated by the following simple example consisting of a so-called shear building, illustrated in Fig. 1. In the example the building has $n = 15$ storeys each with mass $m_0$ and separated by connections with stiffness $k_0$. The 15 vibration modes have normalized natural angular frequencies given by

$$\frac{\omega_j}{(k_0/m_0)^{1/2}} \;=\; 2\sin\left(\frac{\pi}{2}\frac{2j-1}{2n+1}\right) \;=\; 0.1013, 0.3029, 0.5013, 0.6946, 0.8808, \cdots$$

The first five mode shapes are shown in Fig. 7. If the figure were extended symmetrically above the upper floor $n = 15$ the extended mode shapes would correspond to a discrete form of 1, 3, 5, 7, 9 half-wavelengths of a sine-function. The shape functions are here normalized with respect to the maximum displacement, occurring at the top floor.

A single vibration absorber of any of the three types considered above is mounted between the base and the first floor. Thus, the device is activated by any of the vibration modes of the building, but will only be in resonance for one selected mode. The design objective is to generate equal modal damping in the two coupled modes generated by the interaction with the resonant device and to attain a specified level of the resulting damping ratio of these two modes. The level $\zeta_{\mathrm{mode}} = 0.05$ is selected corresponding to an equivalent dynamic amplification of 10 at the resonant frequency. Details are given in

Tables 5 and 6 and for modes 1 and 3 respectively, with normalized natural frequencies $\omega_1 = 0.1013$ and $\omega_3 = 0.5013$.

Table 5: 15-story shear building, $n_a = 1$, resonant mode $r = 1$.

Background parameters $\kappa'_r = 7.212$, $\mu'_r = 0.230$. Equivalent damping $\zeta_{\mathrm{mode}} = 0.05$.

| Type | $\mu$ | $\kappa$ | $m'_d/m_d$ | $k'_d/k_d$ | $c'_d/c_d$ | $\omega_d/\omega_r$ | $\zeta_{r1}$ | $\zeta_{r2}$ |
|---|---|---|---|---|---|---|---|---|
| 1 | 0.0204 | 0.0196 | 1 | 1 | 1 | 0.980 | 0.0599 | 0.0233 |
|   |        |        | 1.005 | 1.165 | 1.356 | 1.055 | 0.0490 | 0.0523 |
| 2 | 0.0196 | 0.0204 | 1 | 1 | 1 | 1.020 | 0.0841 | 0.0234 |
|   |        |        | 1.005 | 1.173 | 1.009 | 1.103 | 0.0504 | 0.0505 |
| 3 | 0.0200 | 0.0200 | 1 | 1 | 1 | 1.000 | 0.0720 | 0.0230 |
|   |        |        | 1.005 | 1.169 | 1.187 | 1.079 | 0.0530 | 0.0504 |

Table 6: 15-story shear building, $n_a = 1$, resonant mode $r = 3$.

Background parameters $\kappa'_r = 10.959$, $\mu'_r = 4.429$. Equivalent damping $\zeta_{\mathrm{mode}} = 0.05$.

| Type | $\mu$ | $\kappa$ | $m'_d/m_d$ | $k'_d/k_d$ | $c'_d/c_d$ | $\omega_d/\omega_r$ | $\zeta_{r1}$ | $\zeta_{r2}$ |
|---|---|---|---|---|---|---|---|---|
| 1 | 0.0204 | 0.0196 | 1 | 1 | 1 | 0.980 | 0.0566 | 0.0235 |
|   |        |        | 1.099 | 1.274 | 1.622 | 1.055 | 0.0486 | 0.0533 |
| 2 | 0.0196 | 0.0204 | 1 | 1 | 1 | 1.020 | 0.0766 | 0.0234 |
|   |        |        | 1.095 | 1.288 | 1.199 | 1.107 | 0.0518 | 0.0485 |
| 3 | 0.0200 | 0.0200 | 1 | 1 | 1 | 1.000 | 0.0666 | 0.0231 |
|   |        |        | 1.097 | 1.281 | 1.422 | 1.080 | 0.0537 | 0.0498 |

First the ideal mass ratio $\mu$ and stiffness ratio $\kappa$ are determined without including the effect of the background modes. These are given in columns 2 and 3, and are identical for the different modes. It is seen that the roles of $\mu$ and $\kappa$ are interchanged for devices of type 1 and 2. In the following columns the results are split into two rows. The upper row gives the device tuning frequency $\omega_d$, plus the resulting damping ratio for the two interaction modes, $\zeta_{r1}$ and $\zeta_{r2}$. It is seen that there is a fairly large difference between these damping ratios in all cases due to the simplified single-mode procedure. This indicates an unbalanced design, that is corrected by including the effect of the background modes as shown in Tables 2 and 4. The modification of device stiffness, inertia and damping is introduced via the non-dimensional device background flexibility parameter $\kappa'_r$ and background mass parameter $\mu'_r$. These parameters represent the relative effect of the non-resonant background modes for a device with location given by the integer array $\mathbf{w}$. They depend on the selected resonant mode to be targeted, but

are independent of the particular device configuration. The values of the background parameters $\kappa'_r$ and $\mu'_r$ are given for vibration mode 1 in the first row of Table 5 and for mode 3 in the first row of Table 6. It is seen that for mode 1 the effect of the background modes on the device mass is very small, corresponding to $\mu'_1 \ll 1$. This is typical of the lowest mode of a structure, for which the effect of non-resonant higher modes is dominated by a quasi-static contribution – see e.g. [28, 29]. For vibration mode 3 the background effect of the two lower modes is largely in the form of a mass correction, and thus the background mass factor $\mu'_r$ is typically non-negligible for resonant modes higher than the first. The background flexibility and mass factors $\kappa'_r$ and $\mu'_r$ enter into the factors for stiffness, mass and damping via the combinations $\kappa'_r \kappa$ and $\mu'_r \mu$, respectively. The single-mode mass and stiffness parameters $\mu$ and $\kappa$ only show modest variation between the three device configurations treated here, and thus the background mode correction of device stiffness and mass is largely independent of the device type, but depends considerably on the magnitude of the background coefficients and thereby on the particular targeted resonant mode. In contrast, the device type has a considerable effect on the correction of the device damping coefficient.

It is clear from the Tables 5 and 6 that the present correction procedure for non-resonant background effects improves the balance between the two damping ratios $\zeta_{r1}$ and $\zeta_{r2}$ for all the combinations of device type and resonant mode number. This suggests an improved balance between the peaks of two interaction generated peaks in a frequency response analysis, reducing the maximum dynamic amplification factor. This is illustrated in frequency analyses carried out for a horizontal concentrated load on the top floor for each of the three device types for both resonant mode $r = 1$ and resonant mode $r = 3$. The dynamic amplification factor of the top floor is illustrated for mode 1 as function of the normalized excitation frequency $\omega/\omega_1$ for each of three device types in Figs. 8–10, respectively. The left side of the figure shows the dynamic displacement of the top floor $u_{\text{top}}$ normalized with respect to its static equivalent $u_{\text{stat}}$, and the right side of the figure shows the internal device displacement $u_{\text{dev}} = u_*$ normalized with respect to the same static top floor displacement $u_{\text{stat}}$. The results for each of the three device types are remarkably similar. In the absence of background parameter correction all curves show a strongly dominant left peak. In all three cases the background mode correction balances the two peaks and reduces the structural response to about half of that from the unbalanced single-mode calibration. The effect on the internal device motion is similar, but less dramatic. The resulting response curves correspond closely to an equivalent single-degree-of-freedom model, and it is noted that the response is slightly less due to the direct normalization with respect to the static deformation instead of a more detailed normalization via the equivalent modal load and modal response amplitude.

Similar frequency results are presented for each of the three device types in Figs. 11–13 when calibrated for resonance of mode $r = 3$. The results are normalized with the static displacement from a concentrated force at the top floor, and the amplification curves therefore show considerably lower values that for the previous mode 1 analysis. Around the structural resonance frequency $\omega_3$ the dynamic amplification is similar to that of the previous case with $r = 1$. Also for this mode an initial unbalance for the single-mode calibration with a high single right peak is balanced with two nearly equal peaks with half the amplification of the original peak. However, in the case of the present resonant mode $r = 3$ the dynamic amplification curve for the top floor response exhibit
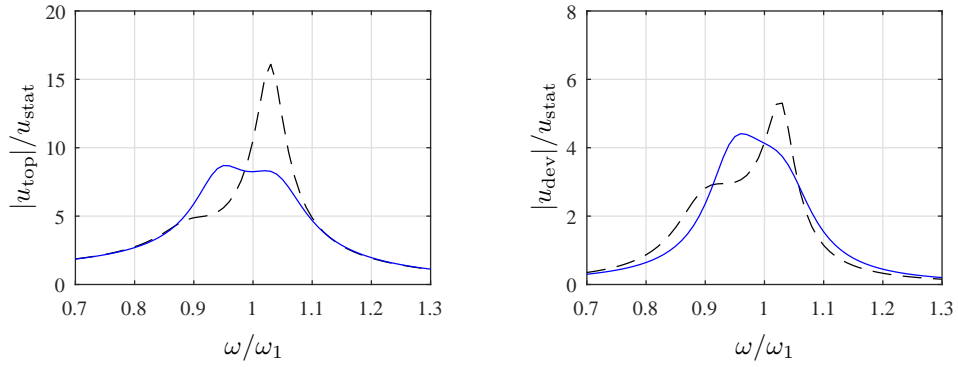
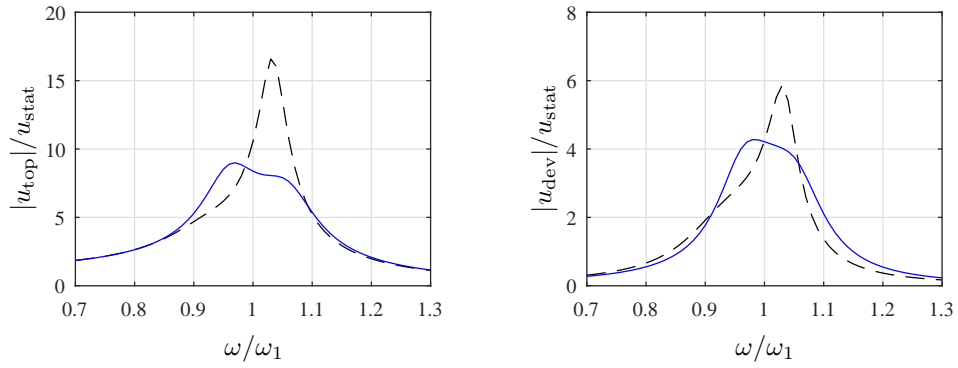Figure 8: Dynamic amplification for mode 1 device type 1. With (—), without (- -) correction.



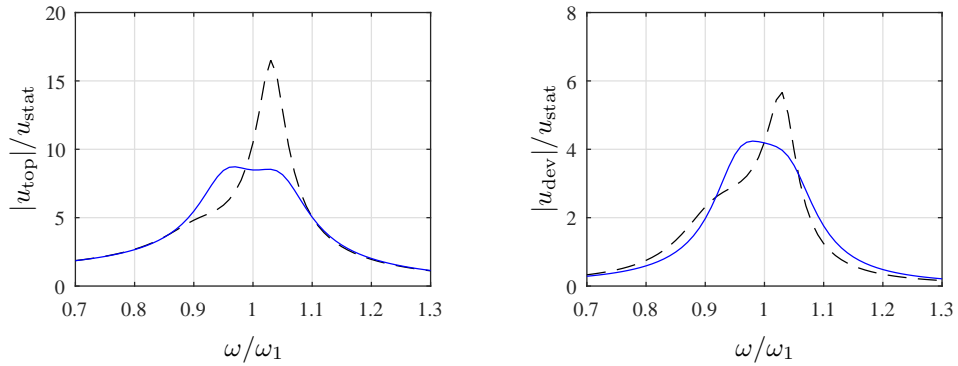Figure 9: Dynamic amplification for mode 1 device type 2. With (—), without (- -) correction.



Figure 10: Dynamic amplification for mode 1 device type 3. With (—), without (- -) correction.
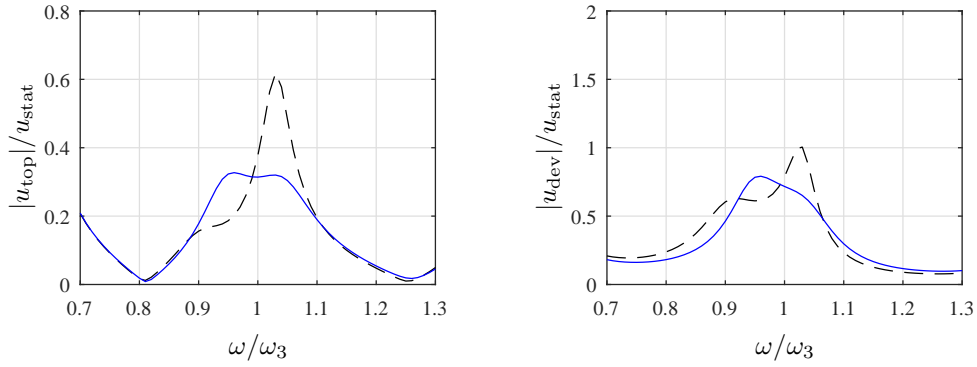
26

Figure 11: Dynamic amplification for mode 3 device type 1. With (—), without (- -) correction.
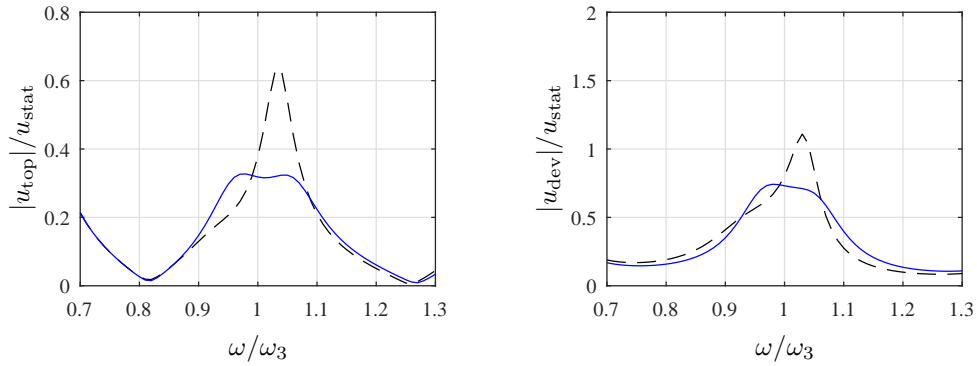


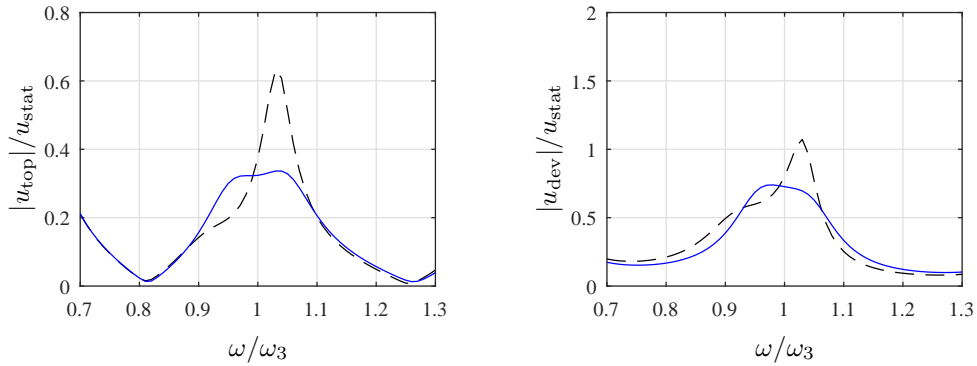Figure 12: Dynamic amplification for mode 3 device type 2. With (—), without (- -) correction.



Figure 13: Dynamic amplification for mode 3 device type 3. With (—), without (- -) correction.

an increase towards both the lower frequencies and the higher frequencies in the graphs. This is due to the closeness of the second mode with relative frequency $\omega_2/\omega_3 \simeq 0.6$ and the fourth mode with relative frequency $\omega_4/\omega_3 \simeq 1.4$. These natural frequencies are only slightly outside the frequency interval in the figure, and as seen from the mode shapes in Fig. 7 the concentrated load at the top floor also excites these modes fairly directly. It is noted that the internal device displacement $u_{\mathrm{dev}}$, which is largely generated by resonance, does not exhibit this effect to a similar extent.

## 7. Conclusions

A theoretical framework for resonant inerter based damping devices on flexible structures has been presented. A central point is that the inerter is activated by the relative motion of its two terminals, and therefore its use on flexible structures often involves the relative motion of two points of the structure. In contrast to tuned mass devices, including the classic tuned mass absorber, a pair of forces acts on two points of a flexible structure and the resulting dynamic response can rarely be described by the response of a single mode. In the present paper a procedure is presented by which the local deformation of the two terminals of the inerter is built from a resonant part containing the relevant resonant mode, plus an additional contribution that lumps the flexibility and inertial effects of the additional local deformation. This effect is a part of the response of the structure to a local pair of opposing forces, operating in resonance with a selected vibration mode, and thus is independent of details of the configuration of the resonant vibration absorber configuration.

The other component of the theoretical framework for resonant damping devices is the formulation of a suitable representation of discrete idealized system with only two degrees-of-freedom. In the present paper three inerter based configurations are considered: an inerter in series with parallel stiffness and damper elements, a stiffness element in series with parallel inerter and damper elements, and finally a series coupling of a stiffness and an inerter element each equipped with a parallel damper element. Each of these idealized devices, as well as several others, allows a simple explicit root locus based design procedure where the key element is the observation that optimal damping properties follow from assuming equal damping ratio of the two modes.

The design procedure for resonant inerter based vibration absorbers on flexible structures consists of a combination of the simple idealized 2 DOF absorber model and an explicit procedure for incorporating the effect of the non-resonant local deformation around the device terminals. The combined procedure is presented in a two-step format, in which the structural system is first represented solely in terms of the properties of the selected resonant mode. The parameters obtained from this single-mode procedure, which is specific for each device type, are subsequently modified to account for the local deformation effects. Examples demonstrate that the performance of the three simple resonant inerter based vibration absorbers are remarkably similar, but that the design parameters depend on the device configuration and on the particular resonant mode. In all the cases considered a nearly optimal balance was attained for the combined device-structure system.

[1] J.P. Den Hartog, *Mechanical Vibrations* (4th edn). McGraw-Hill, New York, 1956. (Reprinted by Dover, New York, 1985)

[2] J.E. Brock, A note on the damped vibration absorber. *Journal of Applied Mechanics*, 13 (1946) A284.

[3] M.C. Smith, Synthesis of mechanical networks: The inerter. *IEEE Transactions on Automatic Control*, 47 (2002) 1648–1662.

[4] M.Z.Q. Chen, C. Papageorgiou, F. Scheibe, F.C. Wang, M.C. Smith, The missing mechanical circuit. *IEEE Circuits and Systems Magazine*, 1531-636X (2009), 10–26.

[5] S. Alessandroni, F. dell'Isola, M.Porfiri, A revival of electric analogs for vibrating mechanical systems aimed to their efficient control by PZT actuators. *International Journal of Solids and Structures*, 39 (2002) 5295–5324.

[6] S. Zhu, W. Shen, X. Qian, Dynamic analogy between an electromagnetic shunt damper and a tuned mass damper. *Smart Materials and Structures*, 22 (2013) 115018 (pp. 11).

[7] S. Krenk, Frequency analysis of the tuned mass damper. *Journal of Applied Mechanics*, 72 (2005) 936–942.

[8] P. Bisegna, G. Caruso, Closed-form formulas for the optimal pole-based design of tuned mass dampers, *Journal of Sound and Vibration*, 331 (2012) 2291–2314.

[9] S.V. Bakre, R.S. Jagid, Optimum parameters of tuned mass damper for damped main system. *Structural Control and Health Monitoring*, 14 (2007) 448–470.

[10] S. Krenk, J. Høgsberg, Tuned mass absorbers on damped structures under random load. *Probabilistic Engineering Mechanics*, 23 (2008) 408–415.

[11] O.F. Tigli, Optimum vibration absorber (tuned mass damper) design for linear damped systems subjected to random load. *Journal of Sound and Vibration*, 331 (2012) 3035–3049.

[12] C. Pan, R. Zhang, Design of structure with inerter system based on stochastic response mitigation ratio. *Structural Control and Health Monitoring*, 25 (2018) e2169 (pp. 21).

[13] Y. Hu, M.Z.Q. Chen, Performance evaluation for inerter-based dynamic vibration absorbers. *International Journal of Mechanical Sciences*, 99 (2015) 297–307.

[14] M. Zilletti, S.J. Elliott, E. Rustighi, Optimisation of dynamic vibration absorbers to minimise kinetic energy and maximise internal power dissipation. *Journal of Sound and Vibration*, 331 (2012) 4093–4100.

[15] K.M. Shum Tuned vibration absorbers with nonlinear viscous damping for damped structures under random load. *Journal of Sound and Vibration*, 346 (2015) 70–80.

[16] I.F. Lazar, S.A. Neild, D.J. Wagg, Using an inerter-based device for structural vibration suppression. *Earthquake Engineering and Structural Dynamics*, 43 (2014) 1129–1147.

[17] Y. Wen, Z. Chen, X. Hua, Design and evaluation of tuned inerter-based dampers for seismic control of MDOF structures. *Journal of Structural Engineering*, 143 (2017) 04016207 (pp. 11).

[18] I.F. Lazar, S.A. Neild, D.J. Wagg, Vibration suppression of cables using tuned inerterdampers. *Engineering Structures*, 122 (2016) 62–71.

[19] L. Sun, D. Hong, L. Chen, Cables interconnected with tuned inerter damper for vibration mitigation. *Engineering Structures*, 151 (2017) 57–67.

[20] X. Shi, S. Zhu, Dynamic characteristics of stay cables with inerter dampers. *Journal of Soundand Vibration*, 423 (2018) 287–305.

[21] S. Krenk, Vibrations of a taut cable with an external damper. *Journal of Applied Mechanics*, 67 (2000) 772–776.

[22] L. Marian, A. Giaralis, Optimal design of a novel tuned mass-damper-inerter (TMDI) passive vibration control configuration for stochastically support-excited structural systems. *Probabilistic Engineering Mechanics*, 38 (2014) 156–164.

[23] A. Giaralis, F. Petrini, Wind-induced vibration mitigation in tall buildings using the tuned mass-damper-inerter. *Journal of Structural Engineering*, 143 (2017) 04017127.

[24] D. De Domenico, G. Ricciardi, An enhanced base isolation system equipped with optimal tuned mass damper inerter. *Earthquake Engineering and Structural Dynamics*, 47 (2018) 1169–1192.

[25] S.Y. Zhang, J.Z. Jiang, S. Neild, Optimal configurations for linear suppression devices in a multi-storey building. *Structural Control and Health Monitoring*, 24 (2017) e1887 (pp. 17).

[26] N.R. Maddox, On the number of modes necessary for accurate response and resulting forces in dynamic analyses. *Journal of Applied Mechanics*, 42 (1975) 516–517.

[27] O.E. Hansteen, K. Bell, Accuracy of mode superposition analysis in structural dynamics. *Earthquake Engineering and Structural Dynamics*, 7 (1979) 405–411.

[28] S. Krenk, J. Høgsberg, Tuned resonant mass absorber on a flexible structure. *Journal of Sound and Vibration*, 333 (2014) 1577–1595.

[29] S. Krenk, J. Høgsberg, Tuned resonant mass or inerter-based absorbers: unified calibration with quasi-dynamic flexibility and inertia correction. *Proceedings of the Royal Society*, A 472 (2016) 20150718.

[30] J. Høgsberg, S. Krenk, Calibration of piezoelectric RL shunts with explicit residual mode correction, *Journal of Sound and Vibration*, 386 (2017) 65–81.